

Characterization of Aldehyde Crosslinked Kenaf Regenerated Cellulose Film

Hatika Kaco,^a Sarani Zakaria,^{a,*} Chin Hua Chia,^a Mohd Shaiful Sajab,^b and Anis Syuhada Mohd Saidi^a

Regenerated cellulose film with better mechanical properties was successfully produced by introducing aldehyde crosslinker during the regeneration process. The cellulose source material was derived from kenaf core powder and dissolved in LiOH/urea solvent at $-13\text{ }^{\circ}\text{C}$ to form a cellulose solution. The cellulose solution was cast and coagulated in a crosslinker bath at different percentages of glutaraldehyde (GA) and glyoxal (GX) to form a regenerated cellulose film. According to Fourier transform infrared spectroscopy (FTIR) spectra, the hydroxyl group of the cellulose was reduced, reducing the percentage of swelling as the percentage of crosslinker was increased. X-ray diffraction (XRD) patterns showed that the crystallinity index of the crosslinked film was decreased. The pore size of the films decreased as the percentage of crosslinker was increased, resulting in decreased film transparency. The pore volume and percentage of swelling in water of the films also increased with decreases in the pore size as the percentage of crosslinker was increased. The tensile strengths of the GA- and GX-crosslinked films increased by 20 and 15% with the addition of 20% of each crosslinker, respectively.

Keywords: Film; Glutaraldehyde; Glyoxal; Pre-cooled method; Tensile strength

Contact information: a: Bioresources and Biorefinery Laboratory, Faculty of Science and Technology, Universiti Kebangsaan Malaysia, 43600 UKM Bangi, Selangor, Malaysia; b: Research Center for Sustainable Process Technology (CESPRO), Faculty of Engineering and Built Environment, Universiti Kebangsaan Malaysia, 43600 UKM Bangi, Selangor, Malaysia;

* Corresponding author: szakaria@ukm.edu.my

INTRODUCTION

Cellulose is the most abundant biopolymer on Earth. It is highly valuable, renewable, biodegradable, bio-compatible, and most importantly, not fully utilized (Luo and Zhang 2010; Zhang *et al.* 2010a). Cellulose is insoluble in most common solvents because of its high density of inter- and intramolecular hydrogen bonds between its hydroxyl groups (Jin *et al.* 2007). Cellulose is found in many lignocellulosic sources; such as cotton linter (Luo and Zhang 2010), wheat straw (Liu *et al.* 2014), oil palm empty fruit bunch fibers (Sajab *et al.* 2014), and kenaf (Mohd Edeerozey *et al.* 2007; Gan *et al.* 2014). The high amounts of cellulose produced every year have been used mainly in the production of paper, panel products, and chemicals industries (Lavoine *et al.* 2012). Like other lignocellulosic fiber, kenaf cellulose is biodegradable and has advantages in the production of plastics and films (Nishino *et al.* 2003). Kenaf is the third largest crop, after wood and bamboo, and has been introduced as a new fiber source capable of being easily modified for industrial purposes, especially in developed countries (Abdul Khalil *et al.* 2010).

There are various solvents used to dissolve cellulose (Chen *et al.* 2006), such as N-methylmorpholine-N-Oxide-water (NMMO/H₂O), lithium chloride/N,N-dimethylacetamide (LiCl/DMAc), and alkali complexes. However, these solvents possess several disadvantages including volatility, toxicity, and high cost (Jin *et al.* 2007). A new, eco-friendly solvent, an alkali/urea system which consists of NaOH/urea, NaOH/thiourea, LiOH/urea, was developed by Zhang and co-workers (2002) to replace previous solvent systems. This solvent system is able to dissolve cellulose at low temperatures (−12 to −13 °C) (Zhang *et al.* 2010a) and can be used to produce various types of products from cellulose, such as hydrogels (Kaco *et al.* 2014a), membranes (Chook *et al.* 2014), films (Kaco *et al.* 2014b), and microbeads (Jin *et al.* 2007).

Previous studies have reported that the properties of the products produced from regenerated cellulose solution *via* the pre-cooled method can be improved by adding epichlorohydrin (ECH) as a crosslinker (Chang *et al.* 2008; Chang *et al.* 2010; Kaco *et al.* 2014a). During the crosslinking process between cellulose and ECH, ether bonds are formed between the hydroxyl groups of cellulose at the C3 and C6 positions to form a crosslinked network; excess ECH turns into glycerol (Chang *et al.* 2008). Previously, several types of aldehyde such as glutaraldehyde (GA) and glyoxal (GX) have been used as crosslinking agents of cellulose fibers (cellulose I) to improve the mechanical properties and reduce water absorption (Rojas and Azevedo 2011). The crosslinking efficiency of GA and GX on cotton fabric was investigated, and it was determined that GA offers better crosslinking properties than GX (Choi *et al.* 1999). However, these crosslinkers have never been reported to produce crosslinked cellulose II products from cellulose solution.

In this study, cellulose was extracted from kenaf core powder by a series of bleaching and alkali treatment processes. The extracted cellulose was dissolved in LiOH/urea solution to produce cellulose solution at low dissolving temperature. Two types of dialdehyde (glutaraldehyde, GA, and glyoxal, GX) were selected as crosslinkers and also functioned as a coagulating bath to produce crosslinked cellulose films. The aim of this study was to introduce aldehyde crosslinkers (GA and GX) to produce crosslinked cellulose films *via* the coagulating method. The effects of the percentage of crosslinker (GA and GX) on the properties of the resulting cellulose films were evaluated. The properties of the crosslinked cellulose films, such as their transparency, morphology, pore volume, swelling, and tensile strength, were also investigated.

EXPERIMENTAL

Materials

Kenaf core (KC) powder was supplied by the Malaysian Agricultural Research and Development Institute (MARDI). Analytical grade lithium hydroxide monohydrate (LiOH·H₂O) and 40% glyoxal (GX) (C₂H₂O₂) were purchased from Sigma Aldrich; urea and 25% glutaraldehyde (GA) (C₅H₈O₂) were purchased from R & M Chemicals; and sodium hydroxide (NaOH) and sulphuric acid (95 to 98% analytical reagent, H₂SO₄) were purchased from System.

Cellulose Extraction

The KC powder was bleached using seven stages of bleaching (D_{Na} E D_{Na} E D_{Na} E D_{Na}) which employed 1.7% sodium chlorite (D_{Na}) and 2% NaOH (E). The sample was treated with each chemical in separate stages, each for 2 h at 80 °C. Afterwards, the KC

powder was washed to remove excess chemicals and dried at 105 °C for 24 h (Kaco *et al.* 2014b). To justify the purity of the extracted cellulose, lignin content after the bleaching sequences was calculated according to TAPPI T 222 os-74 (TAPPI 1978) TAPPI Standard T222. Briefly, samples of KC powder that contained carbohydrates were hydrolyzed with 72%, 24 ± 0.1 N of H₂SO₄ at room temperature for 2 h. The hydrolyzed carbohydrates were solubilized to 3% H₂SO₄ and boiled for 4 h. The insoluble material, which was regarded as lignin, was filtered off, dried, weighed, and the dried lignin was calculated to be 0.3% after the bleaching sequences. The viscosity-average molecular weight of the KC cellulose was 1.68 × 10⁵ (Kaco *et al.* 2014a). It was measured by dissolving the KC cellulose in cadoxen at 25 °C and determined using an Ubbelohde viscometer (Cai *et al.* 2006; Kaco *et al.* 2014a).

Preparation of Crosslinked Cellulose Film

Aqueous LiOH/urea solution, at a weight ratio of 4.6:15, was prepared and stored in a freezer until the temperature reached −13 °C. Bleached KC cellulose powder (3 wt.%) was added into the LiOH/urea solution and stirred for 5 min. The solution was frozen again at −13 °C. This process was repeated three times. The frozen solid was thawed and stirred extensively at room temperature to obtain a transparent cellulose solution. The transparent solution was centrifuged at 8000 rpm for 5 min to remove gas bubbles and separate the undissolved cellulose fraction (Cai *et al.* 2006; Kaco *et al.* 2014b). The undissolved cellulose was calculated and the solubility of cellulose measured was 94.5%.

The cellulose solution produced was cast on a glass plate and coagulated in a distilled water bath containing the crosslinker to obtain the cellulose films after 5 min at room temperature. The film prepared in coagulant without crosslinker was named DI. The coagulants were prepared in a total volume of 1 L at different percentages of crosslinker: 2.5, 5, 10, and 20 wt.% GA (GA2.5, GA5, GA10, and GA20, respectively) and 2.5, 5, 10, and 20 wt.% GX (GX2.5, GX5, GX10, and GX20, respectively). The films were washed with distilled water to remove excess chemicals and air-dried on a PMMA sheet for further characterization.

Characterization

The film samples were analyzed using Attenuated Total Reflectance-Fourier Transform Infrared Spectroscopy (ATR-FTIR) (Perkin Elmer Spectrum 400 FT-IR). X-ray Diffraction (XRD) (Bruker AXS D8 Advance) analysis was performed on the samples using radiation of Cu K α = 1.5458 Å in a diffraction angle (2θ) range of 5 to 60° with a step size of 0.0250°. The surface morphology was studied using a scanning electron microscope (SEM) LEO 1450VP. The sample was sputter-coated with gold before observation.

The swelling percentage of the sample was measured by immersing the film into distilled water until it reached an equilibrium swelling state. The sample was then removed from the distilled water, wiped using filter paper, and weighed. The wet film was dried at 70 °C and re-measured using a moisture analyzer (Moisture Analyzer AND MX-50) until the moisture content was 10%. The percentage of swelling (Q) was calculated using the following equation,

$$Q(\%) = \frac{W_{wet} - W_{dry}}{W_{dry}} \times 100 \quad (1)$$

where Q is the percentage of film swelling, W_{wet} is the weight of the swollen film, and W_{dry} is the weight of the dried film (Li *et al.* 2014).

The pore volume (V_p) of the film was calculated according to Eq. 2,

$$V_p (\%) = \frac{W_{wet} - W_{dry}}{\rho \times W_{dry}} \times 100 \quad (2)$$

where V_p is the pore volume of the film, W_{wet} is the weight of the swollen film, W_{dry} is the weight of the dried membrane, and ρ is the density of water (0.998 g/mL at 30 °C) (Li *et al.* 2014).

The transparency of the cellulose films produced was measured using a UV-Visible Spectrophotometer (Jenway 7315 Spectrophotometer) at wavelengths ranging from 200 to 800 nm. The thickness of the film was approximately 0.015 mm. The tensile properties of the films were measured according to standard test method for Tensile Properties of Thin Plastic Sheeting (ASTM D882) using a Universal Testing Machine (Gotech (Taiwan) AI-3000) at a speed of 10 mm/min. The sample was cut to a size of 50 mm × 10 mm and five replicates were made.

RESULTS AND DISCUSSION

ATR-FTIR and XRD Characterizations

Figure 1 shows the ATR-FTIR spectra of the cellulose films crosslinked at different GA and GX percentages. All major peaks corresponding to cellulose were observed. The broad absorption band observed at 3200 to 3500 cm^{-1} for all samples was attributed to the OH stretching from the intermolecular and intramolecular hydrogen bonds of cellulose (Mansur *et al.* 2008; Qiu and Netravali 2012; Fortunati *et al.* 2013). The band observed between 2880 and 3000 cm^{-1} referred to the stretching of C–H. The peak at 1660 cm^{-1} referred to the bending vibration of residual water molecules in the sample (Kono and Fujita 2012). The band observed at 1430 cm^{-1} was due to the bending vibration of C–H, while the peak at 1150 cm^{-1} referred to the C–O stretching of cellulose (Wu *et al.* 2009). The peak ranging from 894 to 902 cm^{-1} was due to the β -glycosidic linkage (Zhang *et al.* 2002).

The intensities of the peaks at 3200 to 3500 cm^{-1} decreased as the percentage of both GA and GX increased. The relationship between the percentage of crosslinker and the free hydroxyl groups in cellulose can be calculated from the ratio of the area of the O–H band at 3300 cm^{-1} to the bending vibration of C–H at 1460 cm^{-1} . The result is summarized in Table 1. Calculation of the total area for these two bands showed that the ratio of these bands decreased as the percentages of both crosslinkers increased. In the crosslinking reaction, the aldehyde groups from GA and GX will be reacted with hydroxyl group from cellulose, forming hemi-acetal bridges. It has been proposed by other researchers that one aldehyde group links the cellulose chains by reacting with the hydroxyl groups of the cellulose and produces a hemi-acetal structure (Distantina *et al.* 2013; Rojas and Azevedo 2011). Therefore, the aldehyde groups of GA and GX and hydroxyl groups of cellulose have been consumed during the crosslinking reaction. Hence, DI sample with uncrosslinked cellulose has more hydroxyl group compared to crosslinked cellulose. From Table 1, calculation of the total area for O–H band at 3300 cm^{-1} to the bending vibration

of C–H at 1460 cm^{-1} bands showed that the ratio of these bands decreased as the percentages of both crosslinkers increased. This may be due to the increase in the degree of crosslinking and because the availability of hydroxyl groups was reduced (Mansur *et al.* 2008).

Table 1. Ratio of Total Area at 3300 cm^{-1} to 1460 cm^{-1} of Cellulose and Crosslinked Film at Different Percentage of Crosslinker

Sample	Ratio $A_{3300\text{ cm}^{-1}}/A_{1460\text{ cm}^{-1}}$
DI	5.36
GA2.5	5.32
GA5	5.22
GA10	5.14
GA20	4.95
GX2.5	5.30
GX5	5.18
GX10	5.09
GX20	4.94

The peak intensity at 1660 cm^{-1} , attributed to the bending vibration of residual water molecules, decreased as the crosslinker was added to the sample and further decreased as the percentage of crosslinker was increased.

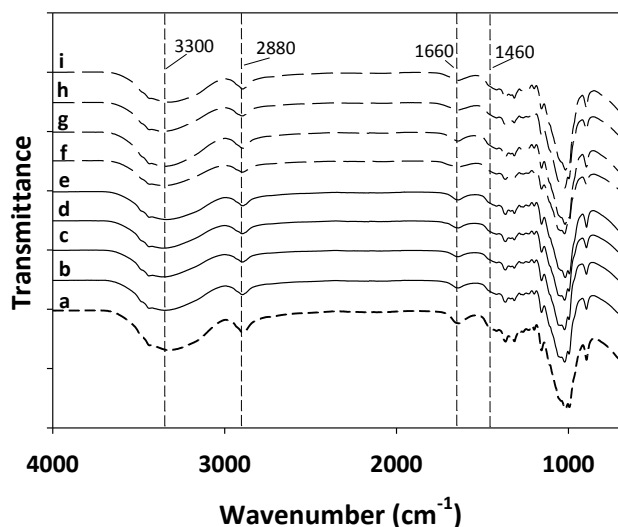


Fig. 1. ATR-FTIR spectra of cellulose films crosslinked with (a) DI, (b) GA 2.5, (c) GA 5, (d) GA10, (e) GA 20, (f) GX2.5, (g) GX5, (h) GX10, and (i) GX20

Figure 2 shows the XRD patterns of cellulose film (DI) and the cellulose films crosslinked with GA and GX. All diffraction patterns exhibited cellulose II crystalline planes of $(1\ \bar{1}\ 0)$, $(1\ 1\ 0)$, and $(2\ 0\ 0)$, and peaks existed at 2θ values of 12.4° , 20.3° , and 22.2° , respectively (Li *et al.* 2012). The crystalline form of native cellulose (cellulose I) which is parallel structure has been converted into cellulose II (antiparallel structure), occurs during dissolution process under alkaline condition (Simon *et al.* 1988). In this case, cellulose swelled due to the reaction with LiOH and therefore, dissolved cellulose. The LiOH penetrates the adjacent amorphous region of cellulose leading to the dissolution of

cellulose. Upon washing and drying, the crystal form of cellulose I was transformed into cellulose II (Kobayashi *et al.* 2011; Simon *et al.* 1988).

The diffraction intensity of both GA and GX crosslinked cellulose films decreased and slightly broadened as compared to the cellulose film coagulated in DI. This is due to the hydrogen bond interaction between the hydroxyl groups of cellulose and aldehyde groups of GA and GX after crosslinking diminished the mobility and disrupted the crystalline arrangement, hence reducing the crystallinity index (CrI) of the film (Choi *et al.* 1999; Acharyulu *et al.* 2013). However, no significant differences were observed in the diffraction patterns or CrI between the two types of crosslinked samples. This demonstrates that both GA and GX possessed similar crystalline arrangements, as far as the diffraction pattern is concerned.

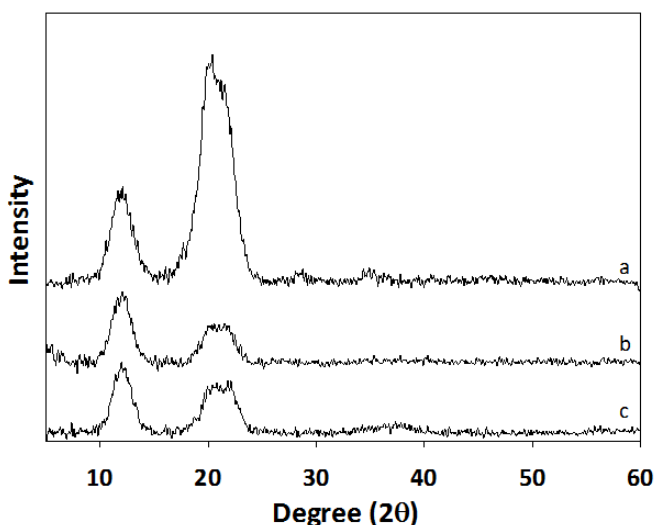
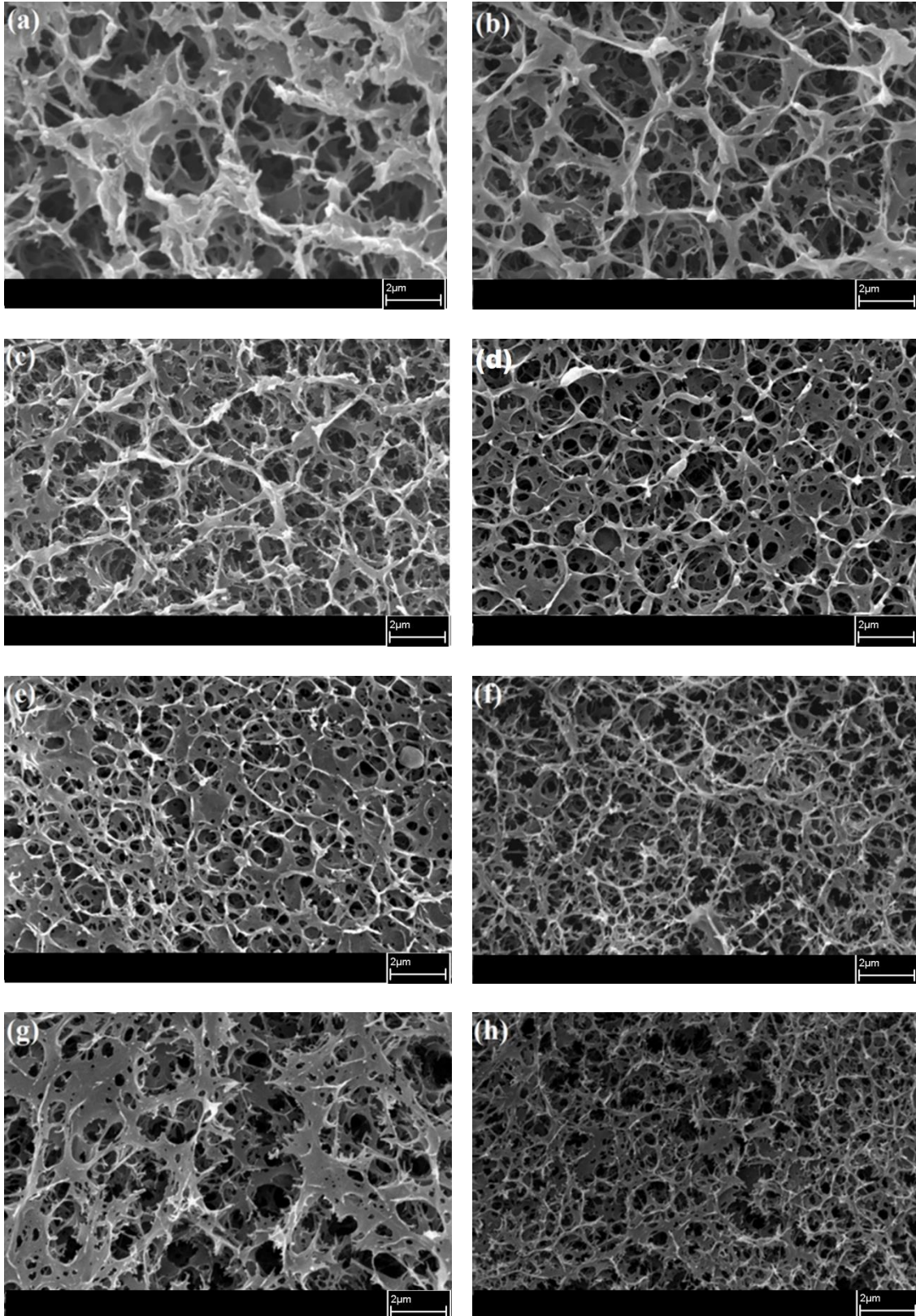


Fig. 2. XRD patterns of cellulose films crosslinked with (a) DI, (b) GX, and (c) GA

Surface Morphology

Figure 3 shows SEM images of the surfaces of all of the cellulose films. Generally, regeneration of cellulose resulted in the formation of a porous structure almost homogeneously scattered over the surface of the films. This indicates that complete regeneration of cellulose occurred (Li *et al.* 2012). During the coagulation process, solvent exchange took place between the cellulose-rich phase and the solvent-rich phase. As the solvent penetrated into the cellulose-rich phase, it created pores on the cellulose regions due to phase separation between the solvent- and cellulose-rich phases, as shown in Fig. 3(a). The same results have been reported by many researchers (Zhang *et al.* 2010b; Li *et al.* 2012; Li *et al.* 2014).

In this system, crosslinking and coagulation processes occurred simultaneously, in which water acted as the coagulant and GA and GX crosslinked with cellulose. However, the addition of different percentages of crosslinker led to different pore sizes. Crosslinking decreased the pore size, as can be seen in Figs. 3(b) to 3(i). As the percentage of crosslinker increased, the pore size decreased. Higher polymer contents led to higher-density polymer chains. This increased intermolecular affinity and further enhanced the driving force of the process (Zhang *et al.* 2010b). Therefore, 10% of GA and GX gave rise to much more dense structures in both crosslinked films.



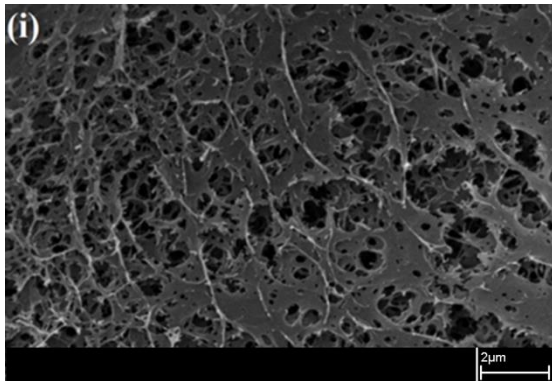


Fig. 3. SEM images of cellulose films crosslinked with (a) DI, (b) GA 2.5, (c) GA 5, (d) GA10, (e) GA 20, (f) GX2.5, (g) GX5, (h) GX10, and (i) GX20

Swelling and Pore Volume

Figure 4 shows the percentage of swelling (Q) of the films against the percentage of crosslinkers used. It shows that as the percentage of crosslinker was increased, Q decreased. The cellulose film without a crosslinker (DI) exhibited the highest Q value, 256%, as compared to those of the crosslinked films (*i.e.*, 164 and 184% for 20% GA and GX, respectively). From the percentage of swelling, the pore volume (V_p) of the cellulose films was calculated and is listed in Figure 5.

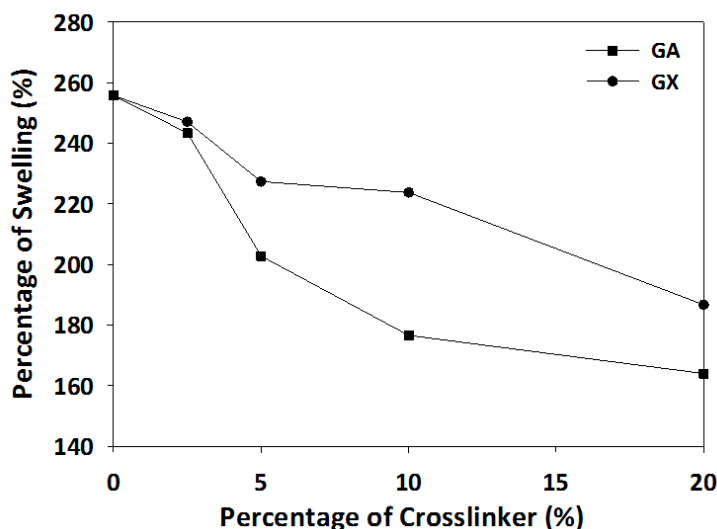


Fig. 4. Degree of swelling of cellulose films against percentage of crosslinker (DI: 0% crosslinker; GA and GX with 2.5 to 20% crosslinker)

The V_p of the DI film was $2.54 \text{ cm}^3/\text{g}$ and the value decreased by 35 and 24% in GA20 and GX20, respectively. The higher percentage of swelling in the DI cellulose film may have been due to the accessibility of the hydroxyl groups in cellulose, which can attract water better than the crosslinked cellulose films. This result is in agreement with Table 1 which shows that the availability of hydroxyl groups was reduced with the increase of the crosslinker percentages. In addition, the lower Q value of the crosslinked cellulose films could be due to the restricted movement of the molecular cellulose chain during the swelling process (Xu *et al.* 2004). Therefore, the percentage of swelling for all films

decreased as the percentage of crosslinker, both GA and GX, was increased (Li *et al.* 2014). Hence, the smaller pore size in the GA- and GX-crosslinked cellulose films influenced their V_p . Cellulose films with higher crosslinker content exhibited lower V_p values. Moreover, the chemical structure of GA possessed a longer chain than GX led to reduce the percentage of pore volume more in GA-crosslinked cellulose film as compared to that of GX-crosslinked film.

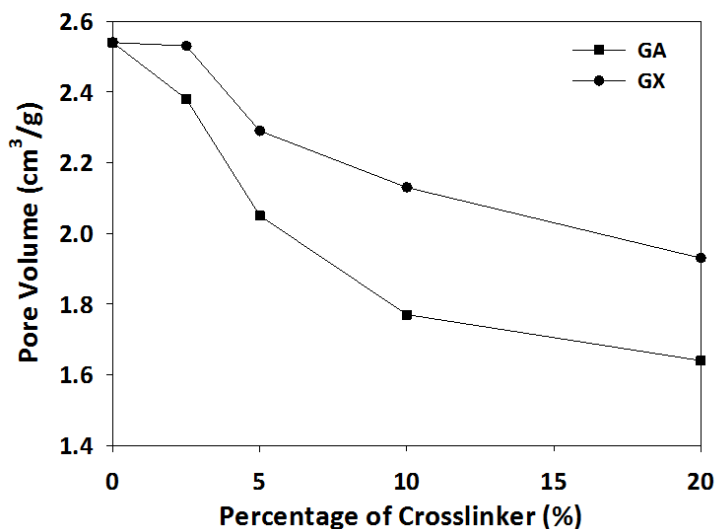


Fig. 5. Pore volume of cellulose films against percentage of crosslinker (DI: 0% crosslinker; GA and GX: 2.5 to 20% crosslinker)

Transparency

Figure 6 shows the light transmittance of the DI film and GA- and GX-crosslinked films. The DI film had a transmittance percentage of 42%, the highest transmittance as compared to those of the crosslinked films. Films containing higher crosslinker percentage exhibited lower transmittances. The light transmittance was reduced further as the amount of crosslinker in the film was increased. The light transmittance may have been affected by the difference in the refractive indexes (RI) of the cellulose and crosslinker. When light reaches an object, it may transmit, reflect, refract, scatter, or absorb the light. In this case, light reflection was more significant when occurring between cellulose and the crosslinker (Tang *et al.* 2011). Equation 3 shows the relationship between light reflection and RI,

$$I = \left[\frac{n_R - n_F}{n_R + n_F} \right]^2 \quad (3)$$

where I is the reflective coefficient, n_R is the RI of GA or GX, and n_F is the RI of cellulose (Li *et al.* 2014). A larger RI difference between cellulose and the crosslinker leads to a higher reflective coefficient; these were about 1.38 and 1.41 for the GA and GX crosslinkers, respectively. It is proposed that there are only cellulose/air interfaces in the DI film. However, after introducing the crosslinker into cellulose/air interfaces, three types of interphases were created (*i.e.*, cellulose/crosslinker, cellulose/air, and crosslinker/air). The increase in the number of interphases could lead to poor light transmission through the films. Furthermore, increasing the percentage of crosslinker resulted in more interphases and reduced light transmission (Althues *et al.* 2007; Tang *et al.* 2011).

GA, with its longer chain, induced more extensive crosslinking with cellulose and hence, a denser structure was formed. Light diffusion into the denser structure was decreased, lowering optical transmittance in cellulose-GA as compared that in the film prepared with the shorter-chain GX (Li *et al.* 2014).

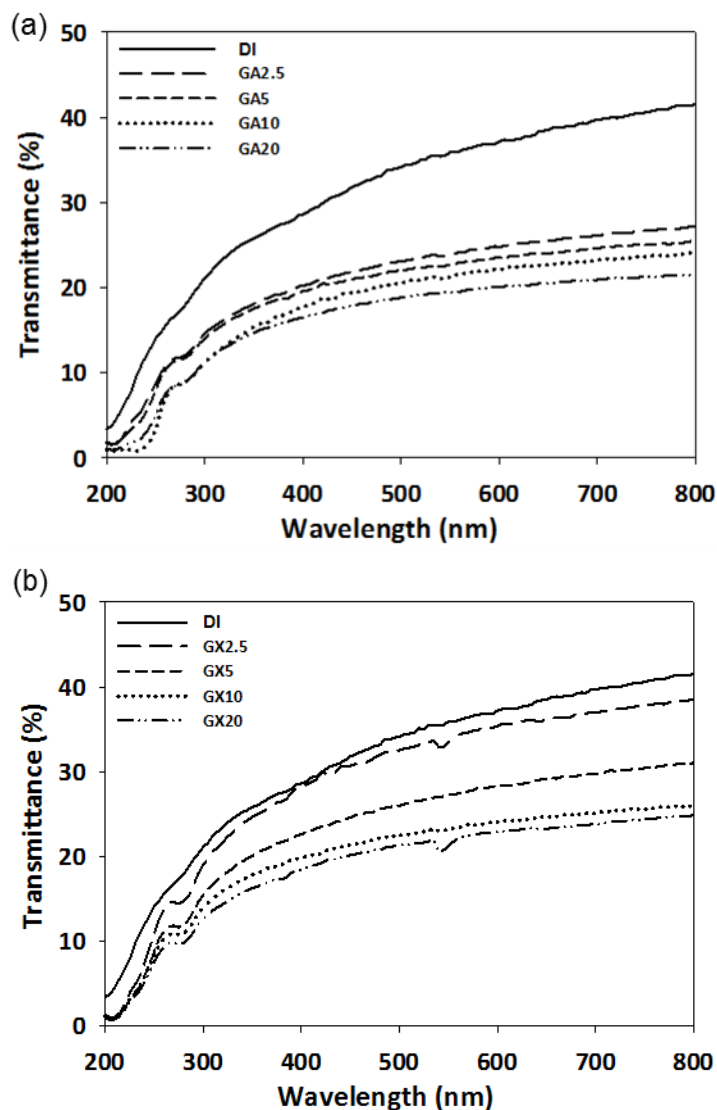


Fig. 6. Light transmittance of cellulose films crosslinked with (a) GA and (b) GX

Tensile Strength

The tensile properties of the DI film and GA- and GX-crosslinked films were tested at room temperature. Figure 7(a) and (b) shows stress-strain curve for both GA and GX cellulose films and the tensile strength of the samples tested (Figure 7c). Higher crosslinker content increased the strength of the films. The DI cellulose film possessed the lowest tensile strength, 56 MPa. Both the GA- and GX-crosslinked films exhibited increased tensile strength with increasing crosslinker percentage up to 20%. This increased the tensile strengths to 75 and 68 MPa in the GA- and GX-crosslinked films, respectively.

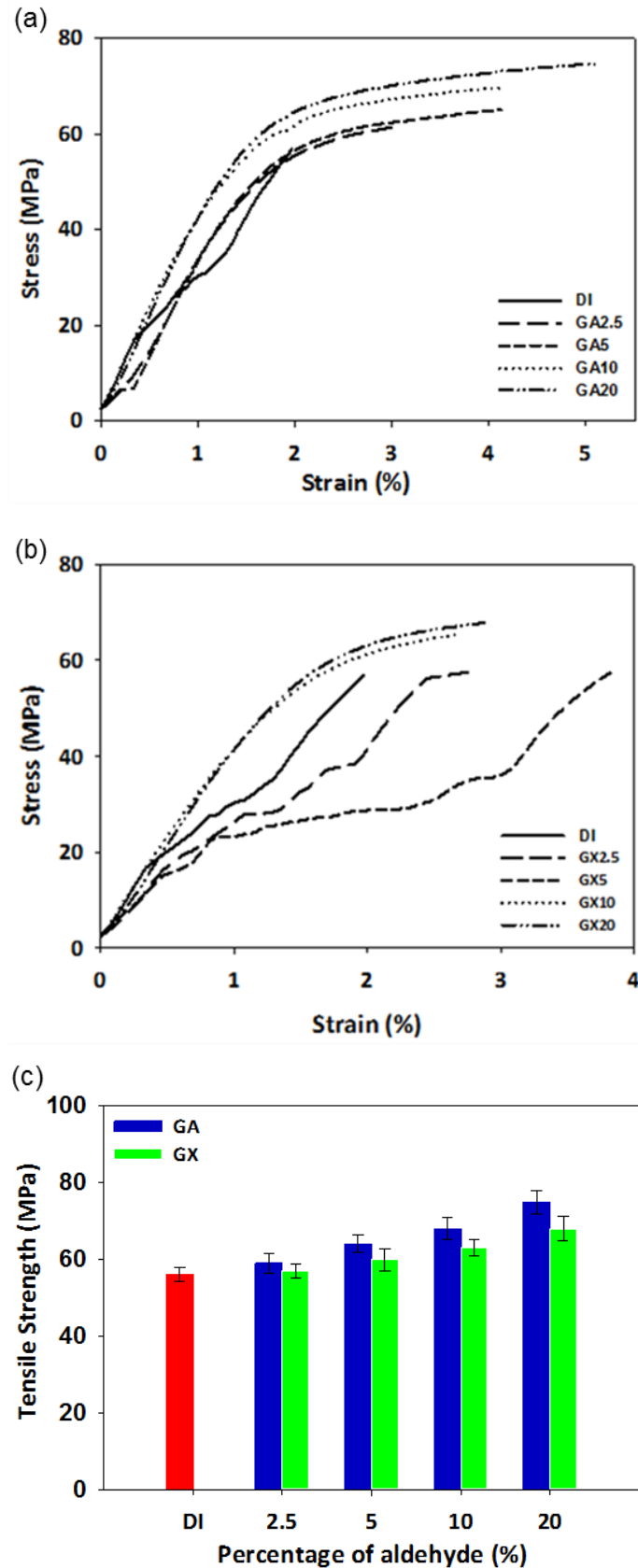


Fig. 7. Stress-strain curve of cellulose films crosslinked with (a) GA, (b) GX, and (c) tensile strength against percentage of aldehyde

The increased tensile strengths suggests that a stronger reaction took place between the cellulose hydroxyl groups and the crosslinker as the percentage of crosslinker increased, as reported earlier from the results of ATR-FTIR (Xu *et al.* 2004; Rojas and Azevedo 2011). Lower pore volume also contributed to higher tensile strength (Li *et al.* 2012), as shown in Fig. 4, in which the pore volume of the crosslinked film was decreased as the percentage of crosslinker was increased. This increased tensile strength in both the GA- and GX-crosslinked films. The GA-crosslinked cellulose films possessed higher tensile strength than those crosslinked with GX. This may be due to the aldehyde group in GX that are close to one another. The effect of steric hindrance was higher, resulting in brittle films. Short crosslinking chains restricted the movement of the cellulose chain due to this brittleness (Rojas and Azevedo 2011).

CONCLUSIONS

1. The number of available hydroxyl groups in cellulose was reduced as the percentage of crosslinker, both glutaraldehyde (GA) and glyoxal (GX), was increased. This reduced the percentage of swelling.
2. X-ray diffraction (XRD) patterns showed that the cellulose film without crosslinker had a higher crystallinity index as compared to those of the GA- and GX-crosslinked films.
3. The addition of different percentages of crosslinker resulted in films with different pore sizes. As the percentage of crosslinker was increased, the pore volume was decreased, which contributed to the reduction in pore size and reduced the light transmittance.
4. The mechanical properties for both cellulose crosslinked with GA and GX were affected. The addition of 20% GX and GA increased the tensile strength of the films by 15 and 20%, respectively. However, the cellulose crosslinked with GA exhibited higher tensile strength as compared to that of GX due to GA's longer molecular chain.

ACKNOWLEDGMENTS

The authors wish to thank Universiti Kebangsaan Malaysia (UKM) for financial support (DIP-2014-013, LRGS/TD/2012/USM-UKM/PT/04, ETP-2013-002) and Centre for Research and Instrumentation Management (CRIM) (UKM) for their equipment and facility support.

REFERENCES CITED

- Abdul Khalil, H. P. S., Yusra, A. F. I., Bhat, A. H., and Jawaid, M. (2010). "Cell wall ultrastructure, anatomy, lignin distribution, and chemical composition of Malaysian cultivated kenaf fiber," *Ind. Crop. Prod.* 31(1), 113-121. DOI: 10.1016/j.indcrop.2009.09.008

- Acharyulu, S. R., Gomathi, T., and Sudha, P. N. (2013). "Synthesis and characterization of cross linked chitosan-polystyrene polymer blends," *Der Pharmacia Lettre*. 5(4), 74-83.
- Althues, H., Henle, J., and Kaskel, S. (2007). "Functional inorganic nanofillers for transparent polymers," *Chem. Soc. Rev.* 36(9), 1454-1465.
DOI: 10.1039/b608177k
- Chang, C., Lue, A., and Zhang, L. (2008). "Effects of crosslinking methods on structure and properties of cellulose/PVA hydrogels," *Macromol. Chem. Physic.* 209(12), 1266-1273. DOI: 10.1002/macp.200800161
- Chang, C., Zhang, L., Zhou, J., Zhang, L., and Kennedy, J. F. (2010). "Structure and properties of hydrogels prepared from cellulose in NaOH/urea aqueous solutions," *Carbohydr. Polym* 82(1), 122-127. DOI: 10.1016/j.carbpol.2010.04.033.
- Chen, X., Burger, C., Fang, D., Zhang, L., Hsiao, B. S., and Chu, B. (2006). "X-ray studies of regenerated cellulose fibers wet spun from cotton linter pulp in NaOH/thiourea aqueous solution," *Polymer* 47(8), 2839-2848.
DOI: 10.1016/j.polymer.2006.02.044
- Chook, S. W., Chia, C. H., Zakaria, S., Ayob, M. K., Huang, N. M., Neoh, H. M., He, M., Zhang, L., and Jamal, R. (2014). "A graphene oxide facilitated highly porous and effective antibacterial regenerated cellulose membrane containing stabilized silver nanoparticles," *Cellulose* 21(6), 4261-4270. DOI: 10.1007/s10570-014-0395-z
- Choi, H. M., Kim, J. H., and Shin, S. (1999). "Characterization of cotton fabrics treated with glyoxal and glutaraldehyde," *J. Appl. Polym. Sci.* 73(13), 2691-2699. DOI: (SICI)1097-4628(19990923)73:13%3C2691::AID-APP17%3E3.3.CO;2-K
- Distantina, S., Rochmadi., Fahrurrozi, M., and Wiratni. (2013) "Preparation and characterization of glutaraldehyde-crosslinked kappa carrageenan hydrogel," *Eng. J. AISC* 17(3), 57-66. DOI: 10.4186/ej.2013.17.3.57.
- Fortunati, E., Puglia, D., Monti, M., Santulli, C., Maniruzzaman, M., and Kenny, J. M. (2013). "Cellulose nanocrystals extracted from okra fibers in PVA nanocomposites," *J Appl Polym Sci* 128(5), 3220-3230. DOI: 10.1002/app.38524
- Gan, S., Zakaria, S., Chia, C. H., Kaco, H., and Mohammad Padzil, F. N. (2014). "Synthesis of kenaf cellulose carbamate using microwave irradiation for preparation of cellulose membrane," *Carbohydr. Polym.* 106, 160-165. DOI: 10.1016/j.carbpol.2014.01.076
- Jin, H., Zha, C., and Gu, L. (2007). "Direct dissolution of cellulose in NaOH/thiourea/urea aqueous solution," *Carbohydr. Res.* 342(6), 851-858. DOI: 10.1016/j.carres.2006.12.023
- Kaco, H., Zakaria, S., Razali, N.F., Chia, C. H., Zhang, L., and Mohamad Jani, S. (2014a). "Properties of cellulose hydrogel from kenaf core prepared via pre-cooled dissolving method," *Sains. Malays.* 43(8), 1221-1229.
- Kaco, H., Zakaria, S., Chia, C. H., and Zhang, L. (2014b). "Transparent and printable regenerated kenaf cellulose/PVA film," *BioResources* 9(2), 2167-2178. DOI: 10.15376/biores.9.2.2167-2178.
- Kobayashi, K., Kimura, S., Togawa, E., and Wada, M. (2011). "Crystal transition from Na-cellulose IV to cellulose II monitored using synchrotron X-ray diffraction," *Carbohydr. Polym* 83(2), 483-488. DOI: 10.1016/j.carbpol.2010.08.006.
- Kono, H., and Fujita, S. (2012). "Biodegradable superabsorbent hydrogels derived from cellulose by esterification crosslinking with 1,2,3,4-butanetetracarboxylic

- dianhydride,” *Carbohydr. Polym.* 87(4), 2582-2588. DOI: 10.1016/j.carbpol.2011.11.045
- Lavoine, N., Desloges, I., Dufresne, A., and Bras, J. (2012). “Microfibrillated cellulose – Its barrier properties and applications in cellulosic materials: A review,” *Carbohydr. Polym.* 90(2), 735-764. DOI: 10.1016/j.carbpol.2012.05.026.
- Li, R., Zhang, L., and Xu, M. (2012). “Novel regenerated cellulose films prepared by coagulating with water: Structure and properties,” *Carbohydr. Polym.* 87(1), 95-100. DOI: 10.1016/j.carbpol.2011.07.023
- Li, W., Wu, Y., Liang, W., Li, B., and Liu, S. (2014). “Reduction of the water wettability of cellulose membrane through controlled heterogeneous modification,” *Appl. Mater. Inter.* 6(8), 5726-5734. DOI: 10.1021/am500341s
- Liu, J., Li, Q., Su, Y., Yue, Q., and Gao, B. (2014). “Characterization and swelling deswelling properties of wheat straw cellulose based semi-IPNs hydrogel,” *Carbohydr. Polym.* 107, 232-240. DOI: 10.1016/j.carbpol.2014.02.073.
- Luo, X., and Zhang, L. (2010). “Creation of regenerated cellulose microspheres with diameter ranging from micron to millimeter for chromatography applications,” *J. Chromatogr. A* 1217(38), 5922-5929. DOI: 10.1016/j.chroma.2010.07.026
- Mansur, H. S., Sadahira, C. M., Souza, A. N., and Mansur, A. A. P. (2008). “FTIR spectroscopy characterization of poly (vinyl alcohol) hydrogel with different hydrolysis degree and chemically crosslinked with glutaraldehyde,” *Mater. Sci. Eng. C* 28(4), 539-548. DOI: 10.1016/j.msec.2007.10.088
- Mohd Edeerozey, A. M., Md Akil, H., Azhar, A. B., and Zainal Ariffin, M. I. (2007). “Chemical modification of kenaf fibers,” *Mater. Lett.* 61(10), 2023-2025. DOI: 10.1016/j.matlet.2006.08.006
- Nishino, T., Hirao, K., Kotera, M., Nakamae, K., and Inagaki, H. (2003). “Kenaf reinforced biodegradable composite,” *Compos. Sci. Technol.* 63(9), 1281-1286. DOI: 10.1016/S0266-3538(03)00099-X
- Qiu, K., and Netravali, A. N. (2012). “Fabrication and characterization of biodegradable composites based on microfibrillated cellulose and polyvinyl alcohol,” *Compos. Sci. Technol.* 72(13), 1588-1594. DOI: 10.1016/j.compscitech.2012.06.010
- Rojas, J., and Azevedo, E. (2011). “Functionalization and crosslinking of microcrystalline cellulose in aqueous media: A safe and economic approach,” *Int. J. Pharm. Sci. Rev. Res.* 8(1), 28-36.
- Sajab, M. S., Chia, C. H., Zakaria, S., and Sillanpää, M. (2014). “Removal of organic pollutants and decolorization of bleaching effluents from pulp and paper mill by adsorption using chemically treated oil palm empty fruit bunch fibers,” *BioResources* 9(3), 4517-4527. DOI: 10.15376/biores.9.3.4517-4527.
- Simon, I., Glasser, L., Scheraga, H. A., and Manley, R. S. J. (1988). “Structure of cellulose. Low-energy crystalline arrangements,” *Macromolecules* 21(4), 990-998. DOI: 10.1021/ma00182a025.
- Tang, C., Wu, M., Wu, Y., Liu, H. (2011). “Effects of fiber surface chemistry and size on the structure and properties of poly (vinyl alcohol) composite films reinforced with electrospun fibers,” *Compos. Part. A* 42(9), 1100-1109. DOI: 10.1016/j.compositesa.2011.04.015.
- TAPPI, 1978c. (1978). “Test Method T 222 os-74. Acid-insoluble in wood and pulp. Technical Report,” *Technical Association for the Pulp and Paper Industries (TAPPI)*

- Wu, R. L., Wang, X. L., Li, F., Li, H. Z., and Wang, Y. Z. (2009). "Green composite films prepared from cellulose, starch and lignin in room-temperature ionic liquid," *Bioresource. Technol.* 100(9), 2569-2574. DOI: 10.1016/j.biortech.2008.11.044
- Xu, G. G., Young, C., and Deng, Y. (2004). "Combination of bifunctional aldehydes and poly(vinyl alcohol) as the crosslinking systems to improve paper wet strength," *J. Appl. Polym. Sci.* 93(4), 1673-80. DOI: 10.1002/app.20593
- Zhang, L., Ruan, D., and Gao, S. (2002). "Dissolution and regeneration of cellulose in NaOH/thiourea aqueous solution," *J. Polym. Sci. Pol. Phys.* 40(14), 1521-1529. DOI: 10.1002/polb.10215
- Zhang, S., Li, F. X., Yu, J. Y., and Hsieh, Y. L. (2010a). "Dissolution behaviour and solubility of cellulose in NaOH complex solution," *Carbohydr. Polym.* 81(3), 668-674. DOI: 10.1016/j.carbpol.2010.03.029
- Zhang, S., Li, F. X., and Yu, J. Y. (2010b). "Kinetics of cellulose regeneration from cellulose-NaOH/thiourea/urea/H₂O system," *Cell. Chem. Technol.* 45(9-10), 593-604.

Article submitted: May 7, 2015; Peer review completed: July 30, 2015; Revised version received and accepted: August 13, 2015; Published: August 19, 2015.

DOI: 10.15376/biores.10.4.6705-6719